ELSEVIER

Contents lists available at ScienceDirect

Ceramics International

journal homepage: www.elsevier.com/locate/ceramint



Origin of unexpected lattice expansion and ferromagnetism in epitaxial $EuTiO_{3-\delta}$ thin films



Run Zhao^{a,*}, Yanda Ji^b, Chao Yang^c, Weiwei Li^d, Yuanyuan Zhu^e, Wei Zhang^f, Hao Lu^a, Yucheng Jiang^a, Guozhen Liu^a, Jiawang Hong^c, Haiyan Wang^g, Hao Yang^{b,**}

- ^a Jiangsu Key Laboratory of Micro and Nano Heat Fluid Flow Technology and Energy Application, College of Mathematics and Physics, Suzhou University of Science and Technology, Suzhou, 215009, China
- ^b College of Science, Nanjing University of Aeronautics and Astronautics, Nanjing, 210016, China
- ^c School of Aerospace Engineering, Beijing Institute of Technology, Beijing, 100081, China
- d Department of Materials Science and Metallurgy, University of Cambridge, 27 Charles Babbage Road, Cambridge, CB3 0FS, UK
- e Department of Materials Science and Engineering, Institute of Materials Science, University of Connecticut, Storrs, CT, 06269, USA
- Hebei Key Laboratory of Optic-Electronic Information Materials, College of Physics Science and Technology, Hebei University, Baoding, 071002, China
- g School of Materials Engineering, Purdue University, West Lafayette, IN, 47907, United States

ARTICLE INFO

Keywords: EuTiO₃₋₈ Vertical lattice expansion Laser energy fluence Antiferromagnetic-ferromagnetic transition

ABSTRACT

This paper uses laser energy fluence as a single variable parameter to investigate the underlying mechanisms that explain the striking physical properties in $EuTiO_{3-\delta}$ ($ETO_{3-\delta}$) thin films. Out-of-plane lattice expansion reveals a linear dependence with laser energy fluence, which induces horizontal cracks near the film/substrate interface. Interestingly, however, by post-annealing the substrate in a hydrogen atmosphere, the planar defects formed during film growth are removed, which suggests that these defects are related to laser energy and are thus created during the deposition. Ferromagnetic order also demonstrates a strong relationship with lattice expansion, which reveals a modulation effect from vertical strain that compensates for the negative effects that result from mixed-valence Eu^{3+} . Ultimately, our results demonstrate that energy-induced defects can be used for manipulating ferromagnetism in antiferromagnetic perovskite systems.

1. Introduction

EuTiO₃ (ETO) is a typical antiferromagnetic-paraelectric (AFM–PE) perovskite oxide with a strong spin-lattice coupling effect [1,2]. In particular, the multiferroic quantum criticality based on the ETO system is particularly useful for exploring the interplay between various types of quantum critical behaviors, which has led to the current attention on this multiferroic material [3]. Considering its significant characteristics, ETO appears to be one of the best candidates for achieving the modification effect of physical properties through different approaches. The first approach is through strain engineering of ferroic behavior [4]. In the past, calculation predictions along with experimental observations of ETO were successful in creating new ferroelectric ferromagnets (FE–FM) from a boring dielectric [5,6]. In the next several years, a variety of research studies focused on understanding octahedral rotation and enhanced multiferroic properties [7–10]. Additionally, doped ions have been used to modify and enhance

FM and FE behavior due to the mixed valence of Eu or Ti ions [11–13]. With further ongoing research, even more significant features, such as the anomalous hall effect and Berry phases in the doped ETO, were discovered under the carrier control [14,15]. But how does the combination of the above tuning effect work in the magnetic behavior of ETO films? More close observation of the competitive and/or cooperative relationships between strain and doping carrier may provide an answer to this question.

To begin to address this question, we need to find a system that contains, simultaneously, both a strain and mixed valence in the ETO. The most suitable system appears to be the as-deposited $ETO_{3-\delta}$ thin films, because they present different magnetic ground states, including AFM and FM. In especially, the films are prepared using different methods. The two most representative deposition processes are pulsed laser deposition (PLD) and molecular beam epitaxy (MBE), which are often used to fabricate epitaxial $ETO_{3-\delta}$ films. The AFM state of unstrained films synthesized by MBE is consistent with that of bulk [16].

E-mail addresses: zhaorun3@gmail.com (R. Zhao), yanghao@nuaa.edu.cn (H. Yang).

^{*} Corresponding author.

^{**} Corresponding author.

This differs from the intrinsic properties of as-grown ETO_{3-δ} thin films grown by PLD, which become FM-like in their behavior, with a Curie temperature around 5 K [17,18]. It is also worth noting that the tuning effect on the magnetic properties is accompanied by the expanded outof-plane spacings in the strained $ETO_{3-\delta}$ films [19]. Accompanied with a strong magnetostriction, the tuned FM order and lattice expansion under a magnetic field have been confirmed in ceramic ETO samples [20,21]. Despite a certain concentration of mixed valence ions, the point defects such as oxygen vacancy and Eu³⁺ alone are insufficient to explain the unexpected properties in ETO films [4]. But returning to the deposition method, the focused laser used in PLD instigates higher kinetic energies in particles, which can then introduce different kinds of defects such as oxygen deficiency in the films. In this paper, we investigate the laser energy fluence that is dependent on the physical properties of the as-deposited $ETO_{3-\delta}$ thin films to understand the underlying mechanisms of them. Our investigation begins after our observation of cracks that seemed to have formed at the substrate/film interface in the as-deposited ETO_{3- δ} films. Furthermore, we discuss how the combination of magnetic measurement and first-principles calculation confirms that the FM intensity is strongly correlated with the stretch of the out-of-plane lattice, which can be seen as arising from the defects that were formed during the film's fabrication.

2. Experimental details

 $ETO_{3-\delta}$ thin films with the same thickness of 130 nm were fabricated on (001)-oriented SrTiO₃ (STO) single-crystal substrates via PLD. A sintered EuTiO3 target was focused by an excimer laser (Lambda Physik, 248 nm, 3 Hz) at varied laser energy fluences from 1 to 3 J/cm² with a laser spot size of 5 mm². The deposition temperature and oxygen pressure were kept at 650 °C and 1 \times 10⁻⁴ Pa, respectively. The films at 3 J/cm² were post-annealed in a reducing atmosphere as indicated by the reference sample [22]. The film c-axis length was determined by an x-ray diffraction (XRD) θ -2 θ scan using a Bruker D8 diffractometer, and the in-plane lattice constant was measured by reciprocal space mapping (RSM) using the Panalytical Empyrean concept. To investigate crystal structures and microstructures, transmission electron microscopy (TEM, FEI Tecnai F20 analytical microscope at 200 kV) was performed. The valence states of the films were confirmed by x-ray photoemission spectroscopy (XPS) at PHI5000 VersaProbe. Magnetic properties of the different films were characterized in a Physical Properties Measurement System (PPMS-9, Quantum Design). We also performed the first-principles calculations in the Vienna ab initio simulation package (VASP) with a plane-wave cutoff of 650 eV for the magnetic properties of the ETO films. An on-site Coulomb parameter U = 5.7 eV and Hund's exchange J = 1.0 eV were selected for the strong electron correlation effects on the f shells of Eu atom, which were well tested in the work of Lee et al. [6]. The I4/mcm structure with the lowest total energy was chosen as the ground state according to our crystal results [23], which was confirmed by many experiment works [7,10,24,25]. The $6 \times 6 \times 6$ Monkhorst and Pack grid of k-point mesh was used for our calculations.

3. Results and discussion

Fig. 1(a) shows the XRD 00l reflection for the STO substrates and films grown at different laser energy fluences. The lattice parameter of the bulk ETO is 3.905 Å [6], which is the same as that of the STO substrates. The separated 00l peaks of the substrates and films indicate that the as-deposited ETO₃₋₈ films with the same thickness exhibit expanded out-of-plane spacings. For example, the c-axis lattice constant increased from 3.940 Å to 4.011 Å when the laser fluence was increased from 1 J/cm $^{-2}$ to 3 J/cm $^{-2}$. Under such conditions, the value of misfit out-of-plane strain in the ETO cells was located in a broad range of +0.89% to +2.71% in a vertical direction. However, different from the lattice expansion along the c-axis, the all in-plane lattice constants in the films were fully fixed to the STO substrate. Fig. 1(c) and (d) present

the representative RSMs around (013) and (103) Bragg peaks of the ETO_{3- δ} film at 3 J/cm². The vertical alignment of the reflections indicates that both the *a*-axis and the *b*-axis lattice parameters of the films were the same as those of the STO substrate. Therefore, under the lower laser energy fluence, the ETO film was found to be closer to stoichiometry. The ϕ scans in Fig. 1(b) show that the ETO phase grows in a cube-on-cube mode on the STO, indicating an epitaxial relation of $(002)_{\rm ETO}//(002)_{\rm STO}$ and $[200]_{\rm ETO}//[200]_{\rm STO}$.

To further understand the origin of vertical lattice expansion, we compared the cross-sectional high resolution TEM (HRTEM) images taken on the (a) film/substrate interface and (b) film. Fig. 2(a) shows that a lateral crack was observed in the interface; vet, no crack propagation occurred into the ETO layer. The direction of the cracks was parallel with the film/substrate interface, likely due to the unique match between ETO/STO along in-plane direction, as opposed to the vertical crack in SrMnO3 films [26]. In contrary, similar cracks and obvious grain boundaries can hardly be observed in the films, as shown in Fig. 2(b). Representative strain maps showing the variation in vertical and lateral strain were determined from a geometric phase analysis (GPA) software in the central and right panels, respectively, and can be seen in Fig. 2(a). It appears that the presence of the two-dimensional dislocations can only increase the out-of-plane lattice constant at the initial deposition, even though it shows negligible influence on the inplane arrangement. Moreover, the out-of-plane lattice parameter remains at the same expansive value throughout the entire thickness of the thin films, with the relaxed in-plane lattice parameter. Therefore, simply increasing the thickness of films can only produce a repetitive effect of lattice expansion rather than actually enlarging it. However, a higher energy fluence can result in the increase of thermal stresses at the interface and, in doing so, produce a crack-extension that appears to enlarge the vertical lattice expansion [27]. The corresponding selectedarea diffraction pattern (Fig. 2(c)) also confirms the lattice expansion and above-mentioned epitaxial relation evidenced by the separated diffraction dots from the ETO₃₋₈/STO. Moreover, previous studies have likewise reported that the post-annealing treatment can be used to relax strain, because the recrystallization process actually repairs the cracks, which seem to vanish at a high temperature, as shown in Fig. 2(d) [18,22].

Fig. 3(a) shows the temperature dependence (T) of the magnetization (M) at varied laser energy fluences. A magnetic field of 100 Oe was applied parallel to the film surface for the measurements. Field cooling (FC) and zero field cooling (ZFC) conditions fell on the same curve for all films (not shown). Aside from the result at the lowest energy density of 1 J/cm^2 , the M of other films increased in a linear relation with decreasing T and appeared to be saturated around 2 K. The monotonical increase in the M-T curves below 4 K indicates that growth-related strain is what accounts for the FM correlation in the ETO_{3-δ} films [13,18]. Furthermore, the comparison of the *M* at 2 K demonstrates that the FM behavior is raised with increasing laser energy fluence. In addition, we fit the derivative of the magnetization (dM/dH) and the inverse susceptibility (χ^{-1}) as a function of temperature to extract the $T_{\rm C}$ of the ferromagnetic $\text{ETO}_{3\text{--}\delta}$ films. This resulted in an interesting effect: when the laser energy fluence is above 1.5 J/cm², a sharp valley in the curve of dM/dH appeared in all the films, as is shown in Fig. 3(c). Combined with the Curie-Weiss law fitting of χ^{-1} (not shown), we found that the $T_{\rm C}$ rose slightly from 3.0 K to 3.7 K, as is presented in the inset of Fig. 3(c). Moreover, it can be observed that the FM order in the ETO₃₋₈ films is enhanced by the strain effect, which is introduced by the change of laser energy fluence.

Clearly, the distinct curve at the lowest energy fluence (1 $\rm J/cm^{-2}$) shows a variation on the magnetic properties among other films. As shown in Fig. 3(b), a comparison of M at 1 $\rm J/cm^{2}$ and the unstrained ETO films determines the magnetic properties under the lowest strain value. Similar to the annealed ETO film, the expanded ETO₃₋₈ film also exhibited a distinct AFM transition at 5.0 K, which is close to the reported temperature in the stoichiometric ETO bulk [2]. However, as

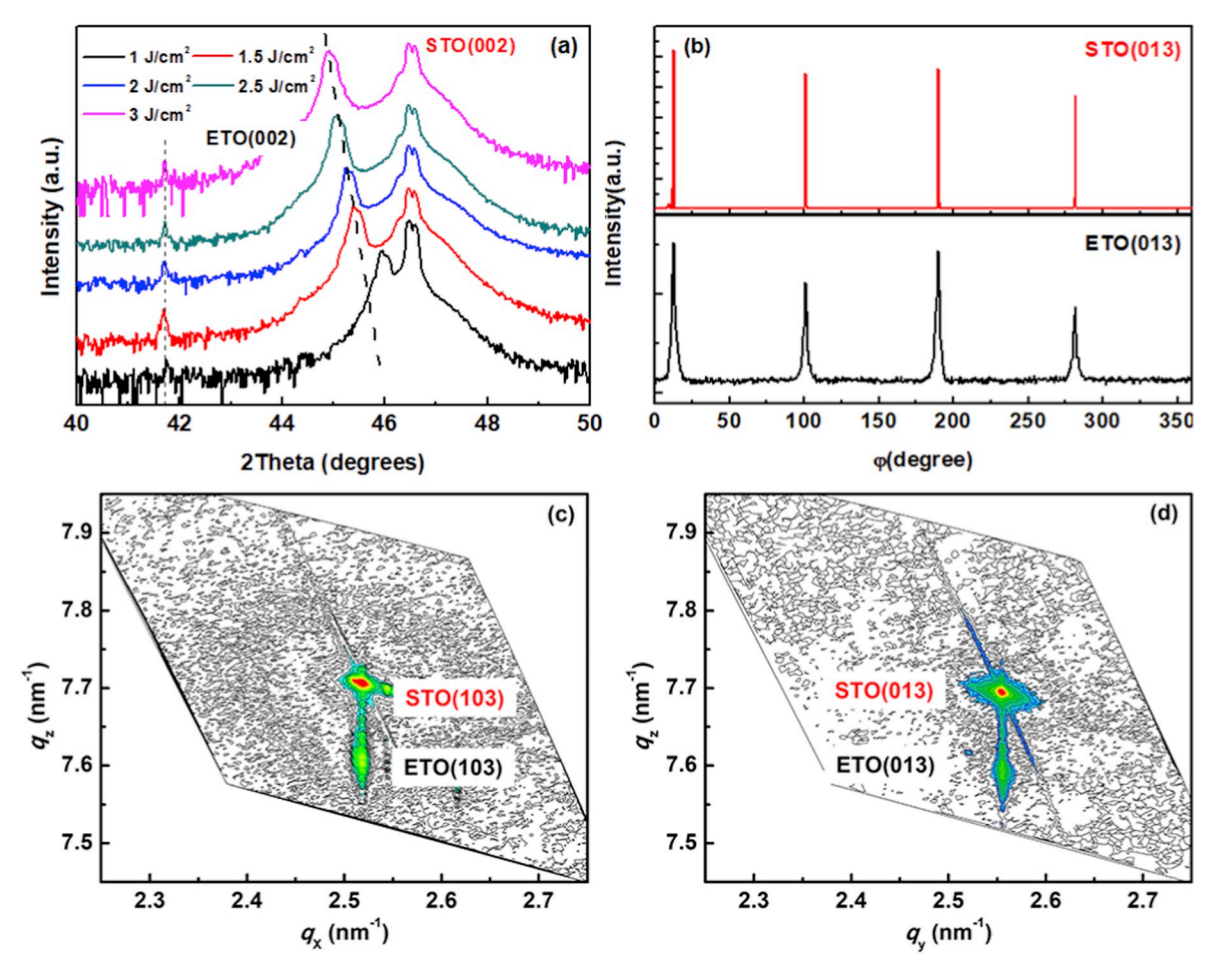


Fig. 1. (a) XRD θ -2 θ scan of the ETO_{3- δ} films grown on STO (001) substrate as a function of laser energy fluence. (b) ϕ scans of the STO (013) (top panel) and the ETO_{3- δ} (013) (bottom panel) reflection. X-ray reciprocal space maps near the (c) (103) and (d) (013) peaks of the STO substrate for an ETO_{3- δ} film.

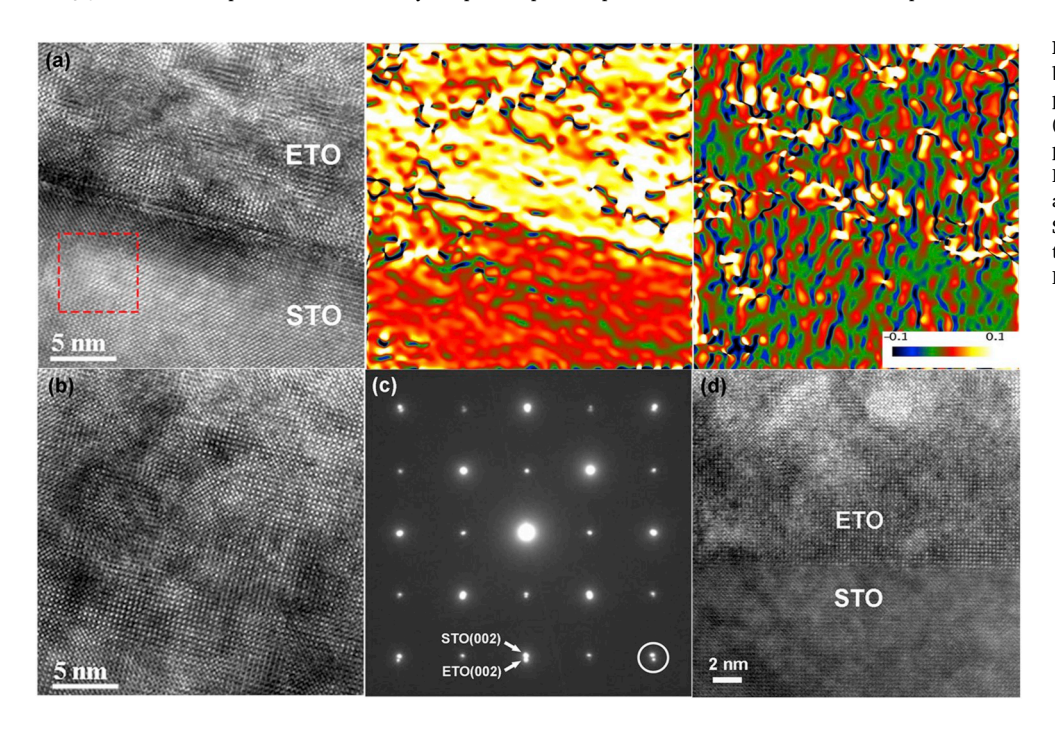


Fig. 2. HRTEM images of (a) the interface between ${\rm ETO_{3-\delta}}/{\rm STO}$ and (b) the as-deposited ${\rm ETO_{3-\delta}}$ film. Maps of out-of-plane (top middle panel) and in-plane (top right panel) strain determined from GPA of HRTEM image (top left panel, the rea dash area was selected as a reference area). (c) Selected-area diffraction (SAD) pattern of the ${\rm ETO_{3-\delta}}$ film and the STO substrate. (d) HRTEM image of the annealed ETO film.

temperature decreases, the change in the M reverses and further increases monotonically around a positive Weiss temperature (θ) of 3.2 K, which is shown as an FM behavior below θ . As shown in our previous

study, the Eu³⁺ defects can be formed in the as-deposited films to compensate the oxygen vacancies that are formed at a high vacuum [22]. More importantly, these nonmagnetic ions can slightly break the

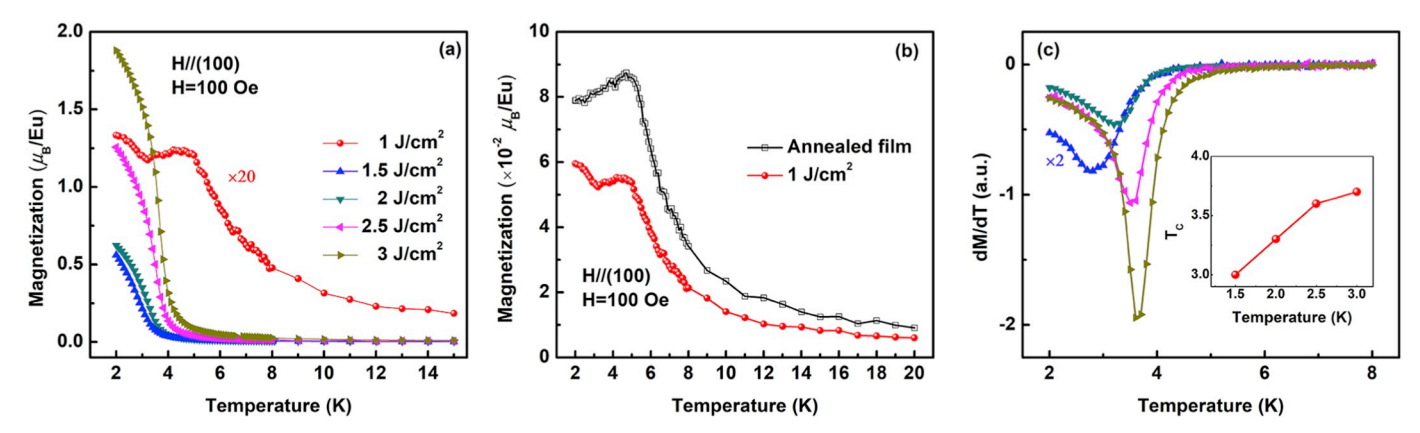


Fig. 3. (a) Temperature dependence of magnetization (M–T) curves under FC condition for the as-deposited ETO_{3- δ} films, at H = 100 Oe. (b) FC magnetization of the annealed ETO film and the ETO_{3- δ} film at 1 J/cm². (c) The derivative of the magnetization with respect to the temperature (obtained from the FC curves) in the FM ETO_{3- δ} films. The inset shows a plot of the ferromagnetic Curie (T_C) temperature *versus* laser energy density.

AFM superexchange magnetic interactions in a vertical direction, which induces a FM interaction at θ rather eliminating the AFM ground state of the ETO_{3–8} films [28].

Fig. 4(a) exhibits the magnetic field (H) dependence of the M measure at 2 K under a different laser energy fluence. The completely different change of M confirms that the AFM and FM phases appear in the various films, respectively. Above 1.5 J/cm², the magnetization increased sharply and then saturated around 5 kOe, which is a process that is party of inherent FM interactions. In contrast, a slower saturation on the magnetization process corresponded to the AFM ground state in

1 J/cm² and in the annealed film. Especially at a low magnetic field, an abrupt increase in slope at 100 Oe caused the magnetization to increase to 4 μ_B /Eu for the film grown under 3 J/cm², relative to the almost unchanged magnetization of 1 J/cm² (Fig. 4(c)). This is because the AFM films require larger magnetic fields for flopping the spin from AFM to FM alignments at Eu site, which is further evident for the strain–induced FM behavior in the ETO3–8 films. Moreover, the saturation M can been seen in the magnified M–H curves in Fig. 4(b). The saturation M in the annealed film (6.79 μ_B /Eu) is close to the theoretical value of 7 μ_B /Eu, which is marked as blue dash in the inset of Fig. 4(b), and

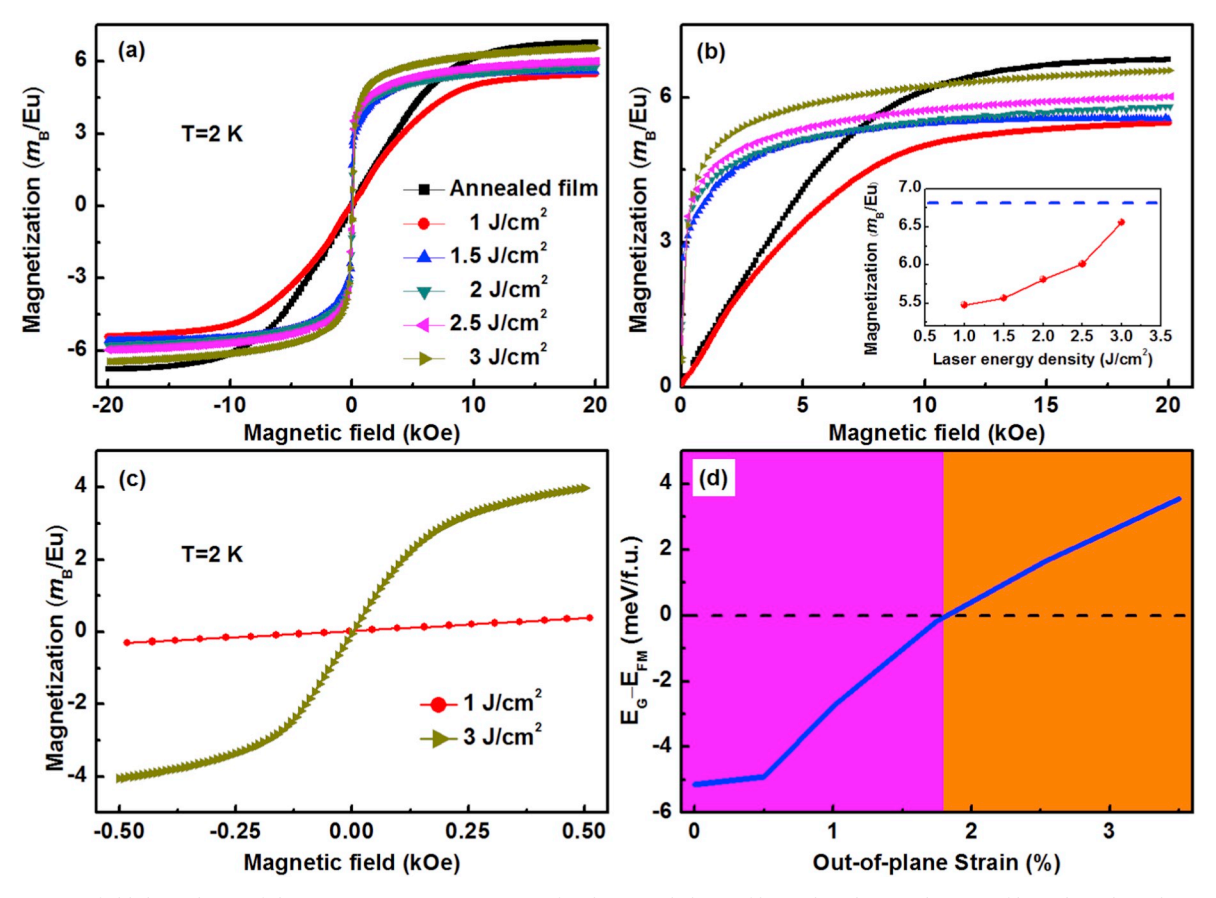


Fig. 4. (a) Magnetic field dependence of the magnetization (M–H) at 2 K for the annealed ETO film and as-deposited ETO_{3- δ} films. (b) Enlarged view of (a). (c) Difference on the M–H curves at the low field between the samples of 1 J/cm² and 3 J/cm². (d) Calculated energy difference between G-AFM and FM states in ETO as a function of the out-of-plane strain. The magenta and orange areas represent G-AFM and FM states, respectively. (For interpretation of the references to colour in this figure legend, the reader is referred to the Web version of this article.)

suggests that the stoichiometric films have the single valence of Eu^{2+} . Moreover, the saturation M of the as-deposited $\mathrm{ETO}_{3-\delta}$ films can been seen to increase with the increase in laser energy fluence from 5.47 $\mu_B/$ Eu to 6.56 μ_B/Eu , indicating that FM behavior can indeed be enhanced by the strain effect, concurrent with the above $M\!-\!T$ results. However, it is worth noting that saturation M of the as-deposited films is smaller than that of the annealed film. This is because the mixed-valence $\mathrm{Eu}^{2+}/\mathrm{Eu}^{3+}$ in the as-deposited films decreases the amount of magnetic moment of the Eu atom and, as a result, reduces saturation M. With an increase in the strain, an increased saturation M represents that the enhanced effect from strain can compensate the negative effect from the nonmagnetic Eu^{3+} ions.

Finally, in order to investigate the underlying mechanism for the tuning effect of out-of-plane strain on magnetic properties, the first-principles density-functional theory (DFT) calculations were carried out. On the basis of the above experiment, in order to simulate the growth-related strain formed during deposition, we stretched the unit-cell along the *c*-axis with a different strain magnitude η and fixed the in-plane lattice at a constant. The energy difference between G-type AFM and FM structures as a function of out-of-plane strain is shown in Fig. 4(d). As is known, the AFM order is favored for unstrained ETO film, which is consistent with many previous investigations [3,5,7,18]. From Fig. 4(d), it can be seen that the G-AFM magnetic structure remains stable at the strain region (η < +1.75%), but that it transfers from a G-AFM to an FE state if the out-of-plane strain is larger than +1.75%, which indicates that FM interactions dominate the spin interaction.

4. Conclusions

In summary, this experiment fabricated as-deposited ETO_{3-δ} and annealed ETO films at different laser energy fluences and observed the striking effects of such changes. From the crystal measurement, the outof-plane lattice constant of the as-deposited films increased with an increase in laser energy fluence, whereas the in-plane lattice constant was fixed to that of the STO substrates. We also found that the unexpected spacing expansion along the c-axis resulted from horizontal cracks that paralleled the film/substrate interface. Furthermore, enhanced FM behavior alongside the expansion was observed when the fluence was above 1.5 J/cm², and the calculated critical strain point of the FM transition was found to be 1.75%. With these findings in mind, we contend that vertical strain can be used to realize AFM-FM phase transition and also to overcome the negative effects that result from nonmagnetic Eu³⁺ ions. Additionally, findings may be helpful for enhancing our understanding of the relationship between strain, defect, and magnetic characteristic in oxide films.

Declaration of competing interest

The authors declare that they have no known competing financial interests or personal relationships that could have appeared to influence the work reported in this paper.

Acknowledgements

The authors acknowledge the support of the National Natural Science Foundation of China (Grant No. 11704272, 11774172, 11704095, 21771136, 11574227, 51802210, 51602152, U1632122, 51502186, 11572040). H.W. acknowledges the TEM support from the US National Science Foundation DMR-1565822. W.L. acknowledges

support from EPSRC grant EP/L011700/1, EP/N004272/1 and the Isaac Newton Trust (Minute 13.38(k)). Theoretical calculations were performed using resources from the National Supercomputer Centre in Guangzhou, which was supported by the Special Program for Applied Research on Super Computation of the NSFC-Guangdong Joint Fund (the second phase) under Grant No. U1501501.

References

- T. Katsufuji, H. Takagi, Coupling between magnetism and dielectric properties in quantum paraelectric EuTiO₃, Phys. Rev. B 64 (2001) 054415.
- [2] T.R. McGuire, M.W. Shafer, R.J. Joenk, H.A. Alperin, S.J. Pickart, Magnetic structure of EuTiO₃, J. Appl. Phys. 37 (1966) 981–982.
- [3] A. Narayan, A. Cano, A.V. Balatsky, N.A. Spaldin, Multiferroic quantum criticality, Nat. Mater. 18 (2019) 223–228.
- [4] D.G. Schlom, L.-Q. Chen, C.J. Fennie, V. Gopalan, D.A. Muller, X. Pan, R. Ramesh, R. Uecker, Elastic strain engineering of ferroic oxides, MRS Bull. 39 (2014) 118–130.
- [5] C.J. Fennie, K.M. Rabe, Magnetic and electric phase control in epitaxial EuTiO₃ from first principles, Phys. Rev. Lett. 97 (2006) 267602.
- [6] J.H. Lee, L. Fang, E. Vlahos, X. Ke, Y.W. Jung, L.F. Kourkoutis, J.-W. Kim, P.J. Ryan, T. Heeg, M. Roeckerath, V. Goian, M. Bernhagen, R. Uecker, P.C. Hammel, K.M. Rabe, S. Kamba, J. Schubert, J.W. Freeland, D.A. Muller, C.J. Fennie, P. Schiffer, V. Gopalan, E. Johnston-Halperin, D.G. Schlom, A strong ferroelectric ferromagnet created by means of spin-lattice coupling, Nature 466 (2010) 954.
- [7] Y. Yang, W. Ren, D. Wang, L. Bellaiche, Understanding and revisiting properties of EuTiO₃ bulk material and films from first principles, Phys. Rev. Lett. 109 (2012) 267602
- [8] V. Goian, S. Kamba, O. Pacherová, J. Drahokoupil, L. Palatinus, M. Dušek, J. Rohlíček, M. Savinov, F. Laufek, W. Schranz, A. Fuith, M. Kachlík, K. Maca, A. Shkabko, L. Sagarna, A. Weidenkaff, A.A. Belik, Antiferrodistortive phase transition in EuTiO₃, Phys. Rev. B 86 (2012) 054112.
- [9] P.J. Ryan, J.W. Kim, T. Birol, P. Thompson, J.H. Lee, X. Ke, P.S. Normile, E. Karapetrova, P. Schiffer, S.D. Brown, C.J. Fennie, D.G. Schlom, Reversible control of magnetic interactions by electric field in a single-phase material, Nat. Commun. 4 (2013) 1334.
- [10] J.-W. Kim, P. Thompson, S. Brown, P.S. Normile, J.A. Schlueter, A. Shkabko, A. Weidenkaff, P.J. Ryan, Emergent superstructural dynamic order due to competing antiferroelectric and antiferrodistortive instabilities in bulk EuTiO₃, Phys. Rev. Lett. 110 (2013) 027201.
- [11] W. Li, Q. He, L. Wang, H. Zeng, J. Bowlan, L. Ling, D.A. Yarotski, W. Zhang, R. Zhao, J. Dai, J. Gu, S. Shen, H. Guo, L. Pi, H. Wang, Y. Wang, I.A. Velasco-Davalos, Y. Wu, Z. Hu, B. Chen, R.-W. Li, Y. Sun, K. Jin, Y. Zhang, H.-T. Chen, S. Ju, A. Ruediger, D. Shi, A.Y. Borisevich, H. Yang, Manipulating multiple order parameters via oxygen vacancies: the case of Eu_{0.5}Ba_{0.5}TiO₃₋₈, Phys. Rev. B 96 (2017) 115105.
- [12] Z.-J. Mo, Q.-L. Sun, C.-H. Wang, H.-Z. Wu, L. Li, F.-B. Meng, C.-C. Tang, Y. Zhao, J. Shen, Effects of Sr-doping on the giant magnetocaloric effect of EuTiO₃, Ceram. Int. 43 (2017) 2083–2088.
- [13] D. Akahoshi, H. Horie, S. Sakai, T. Saito, Ferromagnetic behavior in mixed valence europium ($\mathrm{Eu^{2+}/Eu^{3+}}$) oxide $\mathrm{EuTi_{1-x}M_xO_3}$ (M = $\mathrm{Al^{3+}}$ and $\mathrm{Ga^{3+}}$), Appl. Phys. Lett. 103 (2013) 172407.
- [14] K.S. Takahashi, H. Ishizuka, T. Murata, Q.Y. Wang, Y. Tokura, N. Nagaosa, M. Kawasaki, Anomalous Hall effect derived from multiple Weyl nodes in highmobility EuTiO₃; films, Sci. Adv. 4 (2018) eaar7880.
- [15] K. Ahadi, Z. Gui, Z. Porter, J.W. Lynn, Z. Xu, S.D. Wilson, A. Janotti, S. Stemmer, Carrier density control of magnetism and Berry phases in doped EuTiO₃, Apl. Mater. 6 (2018) 056105.
- [16] J.H. Lee, X. Ke, N.J. Podraza, L.F. Kourkoutis, T. Heeg, M. Roeckerath, J.W. Freeland, C.J. Fennie, J. Schubert, D.A. Muller, P. Schiffer, D.G. Schlom, Optical band gap and magnetic properties of unstrained EuTiO₃ films, Appl. Phys. Lett. 94 (2009) 212509.
- [17] K. Kugimiya, K. Fujita, K. Tanaka, K. Hirao, Preparation and magnetic properties of oxygen deficient EuTiO₃₋₈ thin films, J. Magn. Magn Mater. 310 (2007) 2268–2270.
- [18] K. Fujita, N. Wakasugi, S. Murai, Y. Zong, K. Tanaka, High-quality antiferromagnetic EuTiO₃ epitaxial thin films on SrTiO3 prepared by pulsed laser deposition and postannealing, Appl. Phys. Lett. 94 (2009) 062512.
- [19] Y. Geng, J.H. Lee, D.G. Schlom, J.W. Freeland, W. Wu, Magnetic inhomogeneity in a multiferroic $EuTiO_3$ thin film, Phys. Rev. B 87 (2013) 121109.
- [20] P.G. Reuvekamp, R.K. Kremer, J. Köhler, A. Bussmann-Holder, Spin-lattice coupling induced crossover from negative to positive magnetostriction in EuTiO₃, Phys. Rev. B 90 (2014) 094420.
- [21] A. Bussmann-Holder, J. Köhler, K. Roleder, Z. Guguchia, H. Keller, Unexpected magnetism at high temperature and novel magneto-dielectric-elastic coupling in EuTiO₃: a critical review, Thin Solid Films 643 (2017) 3–6.
- [22] R. Zhao, W.W. Li, L. Chen, Q.Q. Meng, J. Yang, H. Wang, Y.Q. Wang, R.J. Tang, H. Yang, Conduction mechanisms of epitaxial EuTiO₃ thin films, Appl. Phys. Lett.

- 101 (2012) 102901.
- [23] M. Allieta, M. Scavini, L.J. Spalek, V. Scagnoli, H.C. Walker, C. Panagopoulos, S.S. Saxena, T. Katsufuji, C. Mazzoli, Role of intrinsic disorder in the structural phase transition of magnetoelectric EuTiO₃, Phys. Rev. B 85 (2012) 184107.
- [24] J. Köhler, R. Dinnebier, A. Bussmann-Holder, Structural instability of EuTiO₃ from X-ray powder diffraction, Phase Transitions 85 (2012) 949–955.
- [25] D.S. Ellis, H. Uchiyama, S. Tsutsui, K. Sugimoto, K. Kato, D. Ishikawa, A.Q.R. Baron, Phonon softening and dispersion in EuTiO₃, Phys. Rev. B 86 (2012) 220301.
- [26] P. Agrawal, J. Guo, P. Yu, C. Hébert, D. Passerone, R. Erni, M.D. Rossell, Strain-
- driven oxygen deficiency in multiferroic $SrMnO_3$ thin films, Phys. Rev. B 94 (2016) 104101.
- [27] H. ElGazzar, E. Abdel-Rahman, H.G. Salem, F. Nassar, Preparation and characterizations of amorphous nanostructured SiC thin films by low energy pulsed laser deposition, Appl. Surf. Sci. 256 (2010) 2056–2060.
- [28] Y. Lin, E.-M. Choi, P. Lu, X. Sun, R. Wu, C. Yun, B. Zhu, H. Wang, W. Li, T. Maity, J. MacManus-Driscoll, Vertical strain-driven antiferromagnetic to ferromagnetic phase transition in EuTiO₃ nanocomposite thin films, ACS Appl. Mater. Interfaces 12 (2020) 8513–8521.